Mechanics of Advanced Materials and Structures (2015) **22**, 33–43
Copyright © Taylor & Francis Group, LLC
ISSN: 1537-6494 print / 1537-6532 online
DOI: 10.1080/15376494.2014.907949

Exact 3D Thermoelectroelastic Analysis of Piezoelectric Plates through a Sampling Surfaces Method

G. M. KULIKOV and S. V. PLOTNIKOVA

Department of Applied Mathematics and Mechanics, Tambov State Technical University, Tambov, Russian Federation

Received 2 February 2014; accepted 20 March 2014.

The article focuses on the use of the method of sampling surfaces (SaS) to exact three-dimensional (3D) solutions of the steady-state problem of thermoelectroelasticity for piezoelectric laminated plates subjected to thermal loading. The SaS method is based on selecting inside the nth layer I_n not equally spaced SaS parallel to the middle surface of the plate in order to choose temperatures, electric potentials, and displacements of these surfaces as basic plate variables. This permits the representation of the proposed thermopiezoelectric plate formulation in a very compact form. The SaS are located inside each layer at Chebyshev polynomial nodes that improves the convergence of the SaS method significantly. As a result, the SaS method can be applied to 3D exact solutions of thermoelectroelasticity for piezoelectric laminated plates with a specified accuracy using the sufficient number of SaS.

Keywords: thermoelectroelasticity, piezoelectric laminated plate, exact 3D solutions, sampling surfaces method

1. Introduction

Three-dimensional (3D) quasi-static analysis of piezoelectric laminated plates subjected to thermal loading has received considerable attention during the past 20 years [1, 2]. There are at least four approaches to 3D exact solutions of thermoelectroelasticity for piezoelectric plates, namely, the Pagano approach [3–5], the state space approach, the asymptotic approach, and the sampling surfaces (SaS) approach [6, 7]. The first approach was implemented for piezoelectric homogeneous and laminated plates in contributions [8–12]. The most popular state space approach was utilized efficiently in [13–16]. The 3D solution of thermoelectroelasticity for piezoelectric rectangular plates using the asymptotic series expansion was obtained by Cheng and Batra [17]. However, the exact 3D solutions for piezoelectric plates subjected to thermal loading on the basis of the SaS technique cannot be found in the open literature. The present article is intended to fill the gap of knowledge in this research area.

The SaS method has been applied very recently to the exact 3D analysis of elastic, electroelastic, and thermoelastic laminated composite plates and shells in papers [18–23]. As SaS denoted by $\Omega^{(n)1}, \Omega^{(n)2}, \ldots, \Omega^{(n)I_n}$, we choose inner surfaces inside the nth layer and interfaces to introduce temperatures $T^{(n)1}, T^{(n)2}, \ldots, T^{(n)I_n}$; electric potentials $\varphi^{(n)1}, \varphi^{(n)2}, \ldots, \varphi^{(n)I_n}$; and displacement vectors $\mathbf{u}^{(n)1}, \mathbf{u}^{(n)2}, \ldots, \mathbf{u}^{(n)I_n}$ of these surfaces as basic plate variables, where I_n is the total number of SaS of the nth layer ($I_n \geq 3$). Such choice of temperatures, electric potentials, and displacements with the consequent use of Lagrange polynomials of degree $I_n - 1$ in the thickness direction for each layer permits the representation of governing equations of the thermopiezoelectric plate formulation in a very compact form. It is important to mention that the developed approach with the arbitrary number of equally spaced SaS [6] does not work properly with the Lagrange polynomials of high degree because Runge's phenomenon can occur, which yields the wild oscillation at the edges of the interval when the user deals with any specific functions. If the number of equispaced nodes is increased, then the oscillations become even larger. Fortunately, the use of Chebyshev polynomial nodes [7] can help to improve significantly the behavior of Lagrange polynomials of high degree for which the error will go to zero as $I_n \to \infty$.

The origins of using the SaS can be found in contributions [24, 25] in which three, four, and five equally spaced SaS are utilized. It is interesting to note also that in a finite layer method [26], which is the most efficient semi-analytical method for the 3D analysis of simply supported laminated plates and cylindrical shells [27–30], the structure is divided into a number of finite layers following the general layer-wise concept [31–34]. Within each finite layer, the trigonometric functions are employed for in-plane interpolations of displacements in a displacement-based formulation [30] and additionally transverse stresses in a mixed formulation [29], whereas the lower-order Lagrange polynomials with equispaced nodal points are accepted for the interpolation in the thickness

Address correspondence to G. M. Kulikov, Department of Applied Mathematics and Mechanics, Tambov State Technical University, Sovetskaya Street 106, Tambov 392000, Russian Federation. E-mail: kulikov@apmath.tstu.ru
Color versions of one or more of the figures in the article can be found online at www.tandfonline.com/umcm.

direction, i.e., the h-refinement is adopted. Thus, the difference between the SaS method and the finite layer method consists in the following: the p-refinement is used in the former, while the h-refinement is used in the latter. Wu et al. [29, 30] showed that the finite layer method with equally spaced nodal surfaces yields good predictions of the mechanical behavior of composite plates and shells. However, the 3D solutions derived are approximate. To obtain the exact 3D solutions, the p-refinement should be invoked. As pointed out earlier, the SaS method utilizes the Lagrange polynomials of high degree with Chebyshev polynomial nodes that allows one to minimize uniformly the error due to Lagrange interpolation. This fact gives an opportunity to find the exact 3D solutions for thermal laminated composite shells with a prescribed accuracy employing the sufficiently large number of SaS.

The authors restrict themselves to finding five right digits in all examples presented except for section 7.1 with the results of the convergence study. The better accuracy is possible but requires more SaS inside each layer to be taken.

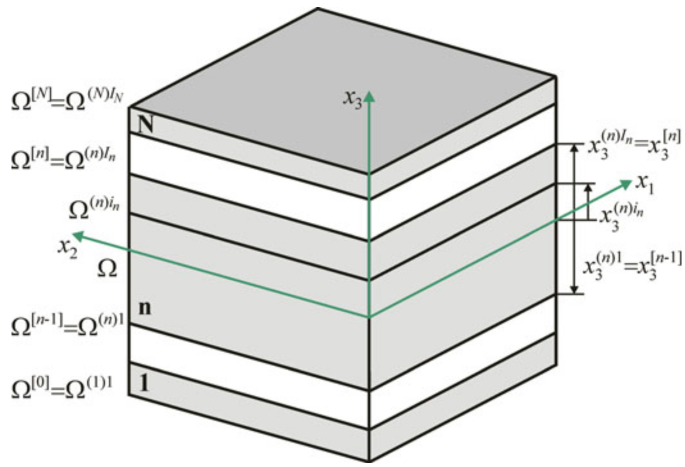

Fig. 1. Geometry of the laminated plate.

2. Description of Temperature Field

Consider a laminated plate of the thickness h. Let the middle surface Ω be described by Cartesian coordinates x_1 and x_2. The coordinate x_3 is oriented in the thickness direction. The transverse coordinates of SaS inside the nth layer are defined as:

$$x_3^{(n)1} = x_3^{[n-1]}, \; x_3^{(n)I_n} = x_3^{[n]}, \tag{1}$$

$$x_3^{(n)m_n} = \frac{1}{2}\left(x_3^{[n-1]} + x_3^{[n]}\right) - \frac{1}{2} h_n \cos\left(\pi \frac{2m_n - 3}{2(I_n - 2)}\right), \tag{2}$$

where $x_3^{[n-1]}$ and $x_3^{[n]}$ are the transverse coordinates of layer interfaces $\Omega^{[n-1]}$ and $\Omega^{[n]}$ depicted in Figure 1; $h_n = x_3^{[n]} - x_3^{[n-1]}$ is the thickness of the nth layer; I_n is the number of SaS corresponding to the nth layer; the index n identifies the belonging of any quantity to the nth layer and runs from 1 to N; N is the total number of layers; the index m_n identifies the belonging of any quantity to the inner SaS of the nth layer and runs from 2 to $I_n - 1$, whereas the indices i_n, j_n, and k_n will be introduced later for describing all SaS of the nth layer run from 1 to I_n. Besides, the tensorial indices i, j, k, l range from 1 to 3 and Greek indices α, β range from 1 to 2.

It is worth noting that the transverse coordinates of inner SaS (2) coincide with the coordinates of Chebyshev polynomial nodes [35]. This fact has a great meaning for a convergence of the SaS method [7].

The relation between the temperature T and the temperature gradient $\mathbf{\Gamma}$ is given by:

$$\mathbf{\Gamma} = \nabla T. \tag{3}$$

In a component form, it can be written as:

$$\Gamma_i = T_{,i}, \tag{4}$$

where the symbol $(\ldots)_{,i}$ stands for the partial derivatives with respect to coordinates x_i.

We start now with the *first assumption* of the proposed thermopiezoelectric laminated plate formulation. Let us assume that the temperature and temperature gradient fields are distributed through the thickness of the nth layer as follows:

$$T^{(n)} = \sum_{i_n} L^{(n)i_n} T^{(n)i_n}, \; x_3^{[n-1]} \le x_3 \le x_3^{[n]}, \tag{5}$$

$$\Gamma_i^{(n)} = \sum_{i_n} L^{(n)i_n} \Gamma_i^{(n)i_n}, \; x_3^{[n-1]} \le x_3 \le x_3^{[n]}, \tag{6}$$

where $T^{(n)i_n}(x_1, x_2)$ are the temperatures of SaS $\Omega^{(n)i_n}$ of the nth layer; $\Gamma_i^{(n)i_n}(x_1, x_2)$ are the components of the temperature gradient at the same SaS; and $L^{(n)i_n}(x_3)$ are the Lagrange polynomials of degree $I_n - 1$ defined as:

$$T^{(n)i_n} = T\left(x_3^{(n)i_n}\right), \tag{7}$$

$$\Gamma_i^{(n)i_n} = \Gamma_i\left(x_3^{(n)i_n}\right), \tag{8}$$

$$L^{(n)i_n} = \prod_{j_n \ne i_n} \frac{x_3 - x_3^{(n)j_n}}{x_3^{(n)i_n} - x_3^{(n)j_n}}. \tag{9}$$

The use of relations (4), (5), (7), and (8) yields:

$$\Gamma_\alpha^{(n)i_n} = T_{,\alpha}^{(n)i_n}, \tag{10}$$

$$\Gamma_3^{(n)i_n} = \sum_{j_n} M^{(n)j_n}\left(x_3^{(n)i_n}\right) T^{(n)j_n}, \tag{11}$$

where $M^{(n)j_n} = L^{(n)j_n}_{,3}$ are the derivatives of Lagrange polynomials, which are calculated at SaS as follows:

$$M^{(n)j_n}\left(x_3^{(n)i_n}\right) = \frac{1}{x_3^{(n)j_n} - x_3^{(n)i_n}} \prod_{k_n \neq i_n, j_n} \frac{x_3^{(n)i_n} - x_3^{(n)k_n}}{x_3^{(n)j_n} - x_3^{(n)k_n}} \text{for } j_n \neq i_n,$$
$$M^{(n)i_n}\left(x_3^{(n)i_n}\right) = -\sum_{j_n \neq i_n} M^{(n)j_n}\left(x_3^{(n)i_n}\right). \tag{12}$$

It is seen from Eq. (11) that the transverse component of the temperature gradient $\Gamma_3^{(n)i_n}$ is represented as a *linear combination* of temperatures of all SaS of the nth layer $T^{(n)j_n}$.

3. Description of Electric Field

The relation between the electric potential φ and the electric field $\mathbf{E}$ is given by:

$$\mathbf{E} = -\nabla\varphi. \tag{13}$$

In a component form, it is expressed as:

$$E_i = -\varphi_{,i}. \tag{14}$$

Following the SaS technique, we introduce now the *second assumption* of the thermopiezoelectric laminated plate formulation. Let the electric potential and the electric field vector be distributed through the thickness of the nth layer similar to temperature distributions (5) and (6), that is,

$$\varphi^{(n)} = \sum_{i_n} L^{(n)i_n}\varphi^{(n)i_n},\ x_3^{[n-1]} \leq x_3 \leq x_3^{[n]}, \tag{15}$$
$$E_i^{(n)} = \sum_{i_n} L^{(n)i_n} E_i^{(n)i_n},\ x_3^{[n-1]} \leq x_3 \leq x_3^{[n]}, \tag{16}$$

where $\varphi^{(n)i_n}(x_1, x_2)$ are the electric potentials of SaS of the nth layer; $E_i^{(n)i_n}(x_1, x_2)$ are the components of the electric field vector at the same SaS defined as:

$$\varphi^{(n)i_n} = \varphi(x_3^{(n)i_n}), \tag{17}$$
$$E_i^{(n)i_n} = E_i(x_3^{(n)i_n}). \tag{18}$$

The use of Eqs. (14), (15), (17), and (18) yields:

$$E_\alpha^{(n)i_n} = -\varphi_{,\alpha}^{(n)i_n}, \tag{19}$$
$$E_3^{(n)i_n} = -\sum_{j_n} M^{(n)j_n}\left(x_3^{(n)i_n}\right)\varphi^{(n)j_n}. \tag{20}$$

One can see that Eq. (20) is similar to Eq. (11). Thus, the transverse component of the electric field $E_3^{(n)i_n}$ is represented as a linear combination of electric potentials of SaS of the nth layer $\varphi^{(n)j_n}$.

4. Description of Mechanical Field

The strain components ε_{ij} are written as:

$$2\varepsilon_{ij} = u_{i,j} + u_{j,i}, \tag{21}$$

where u_i are the displacements of the plate.

Following the SaS technique, we introduce the *third assumption* of the thermopiezoelectric laminated plate formulation developed. Let us assume that displacement and strain distributions through the thickness of the nth layer are similar to thermal and electric field distributions (5), (6), (15), and (16). Thus, we have:

$$u_i^{(n)} = \sum_{i_n} L^{(n)i_n} u_i^{(n)i_n},\ x_3^{[n-1]} \leq x_3 \leq x_3^{[n]}, \tag{22}$$
$$\varepsilon_{ij}^{(n)} = \sum_{i_n} L^{(n)i_n}\varepsilon_{ij}^{(n)i_n},\ x_3^{[n-1]} \leq x_3 \leq x_3^{[n]}, \tag{23}$$

where $u_i^{(n)i_n}(x_1, x_2)$ are the displacements of SaS $\Omega^{(n)i_n}$; $\varepsilon_{ij}^{(n)i_n}(x_1, x_2)$ are the strains of the same SaS defined as:

$$u_i^{(n)i_n} = u_i\left(x_3^{(n)i_n}\right), \tag{24}$$
$$\varepsilon_{ij}^{(n)i_n} = \varepsilon_{ij}\left(x_3^{(n)i_n}\right). \tag{25}$$

Using Eqs. (21), (22), (24), and (25), one obtains:

$$2\varepsilon_{\alpha\beta}^{(n)i_n} = u_{\alpha,\beta}^{(n)i_n} + u_{\beta,\alpha}^{(n)i_n}, \tag{26}$$
$$2\varepsilon_{\alpha3}^{(n)i_n} = \beta_\alpha^{(n)i_n} + u_{3,\alpha}^{(n)i_n}, \tag{27}$$
$$\varepsilon_{33}^{(n)i_n} = \beta_3^{(n)i_n}, \tag{28}$$
$$\beta_i^{(n)i_n} = u_{i,3}(x_3^{(n)i_n}), \tag{29}$$

where $\beta_i^{(n)i_n}(x_1, x_2)$ are the values of derivatives of displacements with respect to transverse coordinate at SaS defined as:

$$\beta_i^{(n)i_n} = \sum_{j_n} M^{(n)j_n}\left(x_3^{(n)i_n}\right)u_i^{(n)j_n}. \tag{30}$$

This means that the key functions $\beta_i^{(n)i_n}$ of the proposed thermopiezoelectric laminated plate formulation are represented as a linear combination of displacements of SaS of the nth layer $u_i^{(n)j_n}$.

5. Variational Formulation of Heat Conduction Problem

The variational equation for the laminated plate can be written as:

$$\delta J = 0, \tag{31}$$

where J is the basic functional of the heat conduction theory given by:

$$J = \frac{1}{2}\int\int_{\Omega}\sum_{n}\int_{x_3^{[n-1]}}^{x_3^{[n]}} q_i^{(n)}\Gamma_i^{(n)} dx_1 dx_2 dx_3 - \int\int_{\hat{\Omega}}\left[\hat{q}_{\mathrm{n}} T + \frac{1}{2}\hat{\mu}(T-\hat{T})^2\right] d\Omega, \qquad (32)$$

where $q_i^{(n)}$ is the heat flux vector of the nth layer; $\hat{q}_{\mathrm{n}}$ is the specified heat flux on the boundary surface $\hat{\Omega}$; $\hat{\mu}$ is the convective heat transfer coefficient; $\hat{T}$ is the reference temperature for convective transfer; and $\hat{\Omega}$ is a part of outer surfaces.

Substituting the temperature gradient distribution (6) into functional (32) and introducing heat flux resultants:

$$Q_i^{(n)i_n} = \int_{x_3^{[n-1]}}^{x_3^{[n]}} q_i^{(n)} L^{(n)i_n} dx_3, \qquad (33)$$

one finds that

$$J = \frac{1}{2}\int\int_{\Omega}\sum_{n}\sum_{i_n} Q_i^{(n)i_n}\Gamma_i^{(n)i_n} dx_1 dx_2 - \int\int_{\hat{\Omega}}\left[\hat{q}_{\mathrm{n}} T + \frac{1}{2}\hat{\mu}(T-\hat{T})^2\right] d\Omega. \qquad (34)$$

Now, we accept the *forth assumption* of the proposed thermopiezoelectric laminated plate formulation. Let the constitutive equations be the Fourier's heat conduction equations:

$$q_i^{(n)} = -k_{ij}^{(n)}\Gamma_j^{(n)},\ x_3^{[n-1]} \le x_3 \le x_3^{[n]}, \qquad (35)$$

where $k_{ij}^{(n)}$ are the components of the thermal conductivity tensor of the nth layer.

Substituting the constitutive Eqs. (35) into Eq. (33) and accounting for the through-the-thickness distribution (6), we obtain:

$$Q_i^{(n)i_n} = -\sum_{j_n}\Lambda^{(n)i_n j_n} k_{ij}^{(n)}\Gamma_j^{(n)j_n}, \qquad (36)$$

where

$$\Lambda^{(n)i_n j_n} = \int_{x_3^{[n-1]}}^{x_3^{[n]}} L^{(n)i_n} L^{(n)j_n} dx_3. \qquad (37)$$

6. Variational Formulation of Thermoelectroelastic Problem

The variational equation for the thermoelectroelastic laminated plate in the case of conservative loading can be written as:

$$\delta\Pi = 0, \qquad (38)$$

where Π is the basic functional of the theory of thermopiezoelectricity given by:

$$\Pi = \frac{1}{2}\int\int_{\Omega}\sum_{n}\int_{x_3^{[n-1]}}^{x_3^{[n]}}\left(\sigma_{ij}^{(n)}\varepsilon_{ij}^{(n)} - D_i^{(n)}E_i^{(n)} - \eta^{(n)}\Theta^{(n)}\right) \times dx_1 dx_2 dx_3 - W, \qquad (39)$$

$$W = \int\int_{\Omega}\left(p_i^+ u_i^{[N]} - p_i^- u_i^{[0]} - \hat{Q}^+\varphi^{[N]} - \hat{Q}^-\varphi^{[0]}\right) \times dx_1 dx_2 + W_{\Sigma}, \qquad (40)$$

where $\sigma_{ij}^{(n)}$ is the stress tensor of the nth layer; $D_i^{(n)}$ is the electric displacement vector of the nth layer; $\eta^{(n)}$ is the entropy density of the nth layer; $u_i^{[0]} = u_i^{(1)1}$ and $u_i^{[N]} = u_i^{(N)I_N}$ are the displacements of bottom and top surfaces $\Omega^{[0]}$ and $\Omega^{[N]}$; $\varphi^{[0]} = \varphi^{(1)1}$ and $\varphi^{[N]} = \varphi^{(N)I_N}$ are the electric potentials of bottom and top surfaces; p_i^- and p_i^+ are the loads acting on outer surfaces; $\hat{Q}^-$ and $\hat{Q}^+$ are the specified electric charges on outer surfaces; W_{Σ} is the work done by external loads applied to the edge surface Σ; $\Theta^{(n)}$ is the temperature rise from the initial reference temperature T_0 defined as:

$$\Theta^{(n)} = T^{(n)} - T_0. \qquad (41)$$

Substituting the electric field and strain distributions (16) and (23) and the temperature distribution:

$$\Theta^{(n)} = \sum_{i_n} L^{(n)i_n}\Theta^{(n)i_n},\ x_3^{[n-1]} \le x_3 \le x_3^{[n]}, \qquad (42)$$

$$\Theta^{(n)i_n} = \Theta\left(x_3^{(n)i_n}\right), \qquad (43)$$

which follows directly from Eqs. (5), (7), and (41) into functional (39), and introducing stress resultants:

$$H_{ij}^{(n)i_n} = \int_{x_3^{[n-1]}}^{x_3^{[n]}} \sigma_{ij}^{(n)} L^{(n)i_n} dx_3, \qquad (44)$$

electric displacement resultants:

$$R_i^{(n)i_n} = \int_{x_3^{[n-1]}}^{x_3^{[n]}} D_i^{(n)} L^{(n)i_n} dx_3, \qquad (45)$$

and entropy resultants:

$$S^{(n)i_n} = \int_{x_3^{[n-1]}}^{x_3^{[n]}} \eta^{(n)} L^{(n)i_n} dx_3, \qquad (46)$$

one obtains:

$$\Pi = \frac{1}{2}\int\int_{\Omega}\sum_{n}\sum_{i_n}\left(H_{ij}^{(n)i_n}\varepsilon_{ij}^{(n)i_n} - R_i^{(n)i_n}E_i^{(n)i_n} - S^{(n)i_n}\Theta^{(n)i_n}\right) \times dx_1 dx_2 - W. \qquad (47)$$

Finally, we introduce the *fifth assumption* of the thermopiezoelectric laminated plate formulation developed. Let us consider the case of linear thermoelectroelastic materials. Therefore, the constitutive equations [31] are written as follows:

$$\sigma_{ij}^{(n)} = C_{ijk\ell}^{(n)}\varepsilon_{k\ell}^{(n)} - e_{kij}^{(n)}E_k^{(n)} - \gamma_{ij}^{(n)}\Theta^{(n)},\ x_3^{[n-1]} \le x_3 \le x_3^{[n]}, \quad (48)$$

$$D_i^{(n)} = e_{ik\ell}^{(n)}\varepsilon_{k\ell}^{(n)} + \in_{ik}^{(n)} E_k^{(n)} + r_i^{(n)}\Theta^{(n)},\ x_3^{[n-1]} \le x_3 \le x_3^{[n]}, \quad (49)$$

$$\eta^{(n)} = \gamma_{kl}^{(n)}\varepsilon_{kl}^{(n)} + r_k^{(n)}E_k^{(n)} + \chi^{(n)}\Theta^{(n)},\ x_3^{[n-1]} \le x_3 \le x_3^{[n]}, \quad (50)$$

where $C_{ijkl}^{(n)}$ are the elastic constants of the nth layer; $e_{kij}^{(n)}$ are the piezoelectric constants of the nth layer; $\gamma_{ij}^{(n)}$ are the thermal stress coefficients of the nth layer; $\in_{ik}^{(n)}$ are the dielectric constants of the nth layer; $r_i^{(n)}$ are the pyroelectric constants of the nth layer; $\chi^{(n)}$ is the entropy-temperature coefficient of the nth layer defined as:

$$\chi^{(n)} = \rho^{(n)}c_{\mathrm{v}}^{(n)}/T_0, \quad (51)$$

where $\rho^{(n)}$ and $c_{\mathrm{v}}^{(n)}$ are the mass density and specific heat per unit mass at constant volume.

The use of through-the-thickness distributions (16), (23), and (42) in Eqs. (44)–(46) and Eqs. (48)–(50) yields:

$$H_{ij}^{(n)i_n} = \sum_{j_n} \Lambda^{(n)i_n j_n}\left(C_{ijk\ell}^{(n)}\varepsilon_{k\ell}^{(n)j_n} - e_{kij}^{(n)}E_k^{(n)j_n} - \gamma_{ij}^{(n)}\Theta^{(n)j_n}\right), \quad (52)$$

$$R_i^{(n)i_n} = \sum_{j_n} \Lambda^{(n)i_n j_n}\left(e_{ik\ell}^{(n)}\varepsilon_{k\ell}^{(n)j_n} + \in_{ik}^{(n)} E_k^{(n)j_n} + r_i^{(n)}\Theta^{(n)j_n}\right), \quad (53)$$

$$S^{(n)i_n} = \sum_{j_n} \Lambda^{(n)i_n j_n}\left(\gamma_{kl}^{(n)}\varepsilon_{kl}^{(n)j_n} + r_k^{(n)}E_k^{(n)j_n} + \chi^{(n)}\Theta^{(n)j_n}\right). \quad (54)$$

7. 3D Solution for Piezoelectric Plate in Cylindrical Bending

In this section, we study a piezoelectric laminated plate in thermal cylindrical bending. The boundary conditions for the simply supported plate whose edges are electrically grounded and maintained at the reference temperature can be written as:

$$\Theta^{(n)} = \varphi^{(n)} = 0 \text{ at } x_1 = 0 \text{ and } x_1 = a, \quad (55)$$

$$\sigma_{11}^{(n)} = u_2^{(n)} = u_3^{(n)} = 0 \text{at} x_1 = 0 \text{ and } x_1 = a, \quad (56)$$

where a is the width of the plate. To satisfy boundary conditions, we search the analytical solution of the problem by a method of Fourier series expansion:

$$\Theta^{(n)i_n} = \sum_r \Theta_r^{(n)i_n} \sin\frac{r\pi x_1}{a}, \quad (57)$$

$$\varphi^{(n)i_n} = \sum_r \varphi_r^{(n)i_n} \sin\frac{r\pi x_1}{a}, \quad (58)$$

$$u_1^{(n)i_n} = \sum_r u_{1r}^{(n)i_n} \cos\frac{r\pi x_1}{a},\ u_2^{(n)i_n} = 0,$$
$$u_3^{(n)i_n} = \sum_r \mathrm{u}_{3r}^{(n)i_n} \sin\frac{r\pi x_1}{a}, \quad (59)$$

where r is the wave number along the x_1-direction.

Substituting a Fourier series (57) in Eq. (34) and using relations (10), (11), (36), (41), and (43), one obtains:

$$J = \sum_r J_r(\Theta_r^{(n)i_n}). \quad (60)$$

Invoking the variational equation (31), we arrive at the system of linear algebraic equations:

$$\frac{\partial J_r}{\partial \Theta_r^{(n)i_n}} = 0 \quad (61)$$

of order K, where $K = \sum_n I_n - N + 1$. Thus, the temperatures $\Theta_r^{(n)i_n}$ of SaS of the nth layer can be easily found by using a method of Gaussian elimination.

Substituting further Fourier series (57), (58), and (59) in Eq. (47) and allowing for relations (19), (20), (26)–(28), (30),

Table 1. Properties of piezoelectric materials

Material	Cadmium selenide	PZT-5A
C_{1111}, GPa	74.1	99.201
C_{2222}, GPa	74.1	99.201
C_{3333}, GPa	83.6	86.856
C_{1122}, GPa	45.2	54.016
C_{1133}, GPa	39.3	50.778
C_{2233}, GPa	39.3	50.778
C_{2323}, GPa	13.17	21.1
C_{1313}, GPa	13.17	21.1
C_{1212}, GPa	14.45	22.593
γ_{11}, Pa/K	6.21e+05	3.314e+05
γ_{22}, Pa/K	6.21e+05	3.314e+05
γ_{33}, Pa/K	5.51e+05	3.26e+05
e_{311}, C/m^2	−0.16	−7.209
e_{322}, C/m^2	−0.16	−7.209
e_{333}, C/m^2	0.347	15.118
e_{113}, C/m^2	−0.138	12.322
e_{223}, C/m^2	−0.138	12.322
$\in_{11}$, F/m	8.25e–11	1.53e–08
$\in_{22}$, F/m	8.25e–11	1.53e–08
$\in_{33}$, F/m	9.02e–11	1.5e–08
r_3, C/m^{2}K	–2.94e–06	7.0e–04
k_{11}, W/mK	9.0	1.8
k_{22}, W/mK	9.0	1.8
k_{33}, W/mK	13.5	1.8
ρ, Kg/m^3	5810	7650
c_{v}, J/KgK	260	350

Table 2. Results of the convergence study for a single-layer piezoelectric plate with $a/h = 2$ in the case of heat flux boundary conditions

I_1	$\bar{\Theta}(0.5)$	$\bar{\varphi}(0.5)$	$\bar{u}_1(0.5)$	$\bar{u}_3(0)$
3	1.514830974804894	−1.276585132031578	−6.992090213777479	4.039437427219185
7	1.516041850892555	−1.287176996356866	−6.936228360092725	4.045924923554766
11	1.516041850893569	−1.287176996676169	−6.936228359388562	4.045924921944983
15	1.516041850893570	−1.287176996676170	−6.936228359388562	4.045924921942870
19	1.516041850893570	−1.287176996676169	−6.936228359388563	4.045924921942869
23	1.516041850893570	−1.287176996676170	−6.936228359388563	4.045924921942869
27	1.516041850893570	−1.287176996676170	−6.936228359388563	4.045924921942869

and (52)–(54), we find:

$$\Pi = \sum_r \Pi_r \left(u_{1r}^{(n)i_n}, u_{3r}^{(n)i_n}, \varphi_r^{(n)i_n}, \Theta_r^{(n)i_n}\right). \qquad (62)$$

The use of Eqs. (38) and (62) leads to a system of linear algebraic equations:

$$\frac{\partial \Pi_r}{\partial u_{1r}^{(n)i_n}} = 0, \; \frac{\partial \Pi_r}{\partial u_{3r}^{(n)i_n}} = 0, \; \frac{\partial \Pi_r}{\partial \varphi_r^{(n)i_n}} = 0 \qquad (63)$$

of order $3K$. The linear system (63) is solved through a method of Gaussian elimination.

The described algorithm was performed with the Symbolic Math Toolbox, which incorporates symbolic computations into the numeric environment of MATLAB. This in turn gives the possibility to derive the exact solutions of thermoelectroelasticity for laminated anisotropic plates in cylindrical bending with a specified accuracy.

7.1. *Validation of SaS Approach for Heat Flux Boundary Conditions*

As a numerical example, we consider a simply supported single-layer plate composed of cadmium selenide polarized in the thickness direction. The material properties are presented in [8, 36] and Table 1. Let the plate be loaded on the top surface by the sinusoidally distributed heat flux, whereas the bottom surface is assumed to be heat-insulated. The boundary conditions on the top and bottom surfaces are taken to be:

$$\begin{aligned} &q_3^{(1)} = q_0 \sin\tfrac{\pi x_1}{a},\, D_3^{(1)} = \sigma_{13}^{(1)} = \sigma_{23}^{(1)} = \sigma_{33}^{(1)} = 0 \text{ at } x_3 = h/2, \\ &q_3^{(1)} = 0,\, D_3^{(1)} = \sigma_{13}^{(1)} = \sigma_{23}^{(1)} = \sigma_{33}^{(1)} = 0 \text{ at } x_3 = -h/2, \end{aligned} \qquad (64)$$

where $a = 1$m, $q_0 = 1$W/m^2, and $T_0 = 293$K. To evaluate the results of the convergence study, we introduce the dimensionless field variables:

$$\begin{aligned} &\bar{\Theta} = 10hk_0\Theta(a/2, z)/a^2 q_0,\, \bar{\varphi} = 10^3 k_0 d_0 \varphi(a/2, z)/a^2\alpha_0 q_0, \\ &\bar{u}_1 = 100hk_0 u_1(0, z)/a^3\alpha_0 q_0, \\ &\bar{u}_3 = 100k_0 u_3(a/2, z)/a^2\alpha_0 q_0,\, z = x_3/h, \end{aligned} \qquad (65)$$

where $\alpha_0 = 4.396 \times 10^{-6}$1/K, $k_0 = 9$W/mK, and $d_0 = 3.9238 \times 10^{-12}$C/N.

The data listed in Tables 2 and 3 show that the SaS method permits the derivation of exact solutions of thermoelectroelasticity for thick piezoelectric plates in cylindrical bending with a high accuracy using the large number of SaS. As it turned out, the SaS method can provide 15 right digits for basic variables at crucial points employing 13 inner SaS inside the plate body. It is important to note that here the bottom and top surfaces are not included into a set of SaS because the use of Chebyshev polynomial nodes allows one to minimize uniformly the error due to Lagrange interpolation.

7.2. *Validation of SaS Approach for Convective Boundary Conditions*

Next, we study the same cadmium selenide plate. To validate this type of thermal loading, we consider boundary conditions on the top and bottom surfaces [8] as follows:

$$\begin{aligned} &\Theta_{,3}^{(1)} + h^+\Theta^{(1)} = h^+\Theta_0 \sin\frac{\pi x_1}{a},\, D_3^{(1)} \\ &\quad = \sigma_{13}^{(1)} = \sigma_{23}^{(1)} = \sigma_{33}^{(1)} = 0 \text{ at } x_3 = h/2, \\ &\Theta_{,3}^{(1)} - h^-\Theta^{(1)} = 0, \\ &D_3^{(1)} = \sigma_{13}^{(1)} = \sigma_{23}^{(1)} = \sigma_{33}^{(1)} = 0 \text{ at } x_3 = -h/2, \end{aligned} \qquad (66)$$

Table 3. Results of the convergence study for a single-layer piezoelectric plate with $a/h = 10$ in the case of heat flux boundary conditions

I_1	$\bar{\Theta}(0.5)$	$\bar{\varphi}(0.5)$	$\bar{u}_1(0.5)$	$\bar{u}_3(0)$
3	1.035337086088057	−1.329936076735578	−4.750069515595288	4.830450207594048
7	1.035337187913652	−1.329961621213969	−4.749949149330288	4.829776282323792
11	1.035337187913652	−1.329961621213969	−4.749949149330288	4.829776282323684
15	1.035337187913653	−1.329961621213969	−4.749949149330288	4.829776282323684
19	1.035337187913652	−1.329961621213969	−4.749949149330288	4.829776282323683

Table 4. Results of the convergence study for a single-layer piezoelectric plate with $a/h = 2$ in the case of convective boundary conditions

I_1	$\bar{\Theta}(-0.5)$	$\bar{\Theta}(0.5)$	$\bar{\varphi}(0.5)$	$\bar{u}_1(0.5)$	$\bar{u}_3(0.5)$	$\bar{\sigma}_{11}(0.5)$	$\bar{\sigma}_{13}(-0.25)$	$\bar{\sigma}_{33}(0)$	$\bar{D}_3(0)$	$\bar{q}_3(0.5)$	$\bar{\eta}(0.5)$
5	0.28881	0.63570	−5.2859	−2.9088	9.9580	−15.682	3.1848	−2.8412	−1.3398	−10.920	3.9685
7	0.28881	0.63570	−5.2859	−2.9087	9.9580	−13.098	3.6968	3.9052	−1.3255	−10.929	3.9685
9	0.28881	0.63570	−5.2859	−2.9087	9.9580	−13.089	3.6938	3.8899	−1.3256	−10.929	3.9685
11	0.28881	0.63570	−5.2859	−2.9087	9.9580	−13.089	3.6938	3.8898	−1.3256	−10.929	3.9685
13	0.28881	0.63570	−5.2859	−2.9087	9.9580	−13.089	3.6938	3.8898	−1.3256	−10.929	3.9685
Dube	0.2888	0.6357	−5.286	−2.909	9.958	−13.09					

where $a = 1\text{m}$, $\Theta_0 = 1\text{K}$, $T_0 = 293\text{K}$, $hh^- = 0.2$, and $hh^+ = 2$.

To evaluate the results of the convergence study, the following dimensionless variables are introduced:

$$\begin{aligned}
\bar{\Theta} &= \Theta(a/2, z)/\Theta_0, \quad \bar{q}_3 = 10aq_3(a/2, z)/Sk_0\Theta_0,\\
\bar{\varphi} &= 10^3 d_0\varphi(a/2, z)/h\alpha_0\Theta_0,\\
\bar{D}_3 &= S^2 D_3(a/2, z)/d_0 E_0\alpha_0\Theta_0,\\
\bar{u}_1 &= 10u_1(0, z)/Sh\alpha_0\Theta_0, \quad \bar{u}_3 = 100u_3(a/2, z)/S^2 h\alpha_0\Theta_0,\\
\bar{\sigma}_{11} &= 10^3 S^2\sigma_{11}(a/2, z)/E_0\alpha_0\Theta_0,\\
\bar{\sigma}_{13} &= 10^3 S^3\sigma_{13}(0, z)/E_0\alpha_0\Theta_0,\\
\bar{\sigma}_{33} &= 10^3 S^4\sigma_{33}(a/2, z)/E_0\alpha_0\Theta_0,\\
\bar{\eta} &= 10^{-3}\eta(a/2, z)/E_0\alpha_0^2\Theta_0, \quad z = x_3/h,
\end{aligned} \tag{67}$$

where $S = a/h$ is the slenderness ratio. The reference material data are taken to be $\alpha_0 = 4.396 \times 10^{-6}1/\text{K}$, $k_0 = 9\text{W/mK}$, $d_0 = 3.9238 \times 10^{-12}\text{C/N}$, and $E_0 = 42.785\text{GPa}$.

Tables 4 and 5 list the results of the convergence study utilizing a various number of SaS I_1 inside the plate body. A comparison with the 3D analytical solution of Dube et al. [8] is also given. The derived results demonstrate convincingly the high potential of the developed thermopiezoelectric plate formulation. It is necessary to mention that due to consideration of boundary conditions (66) the bottom and top surfaces are included into a set of SaS. Figure 2 displays through-the-thickness distributions of the temperature, heat flux, electric potential, electric displacement, transverse displacement, transverse stresses, and entropy for different slenderness ratios a/h employing 11 SaS. As can be seen, the boundary conditions on the bottom and top surfaces for transverse components of the electric displacement vector and stress tensor are satisfied exactly by using the constitutive equations (48) and (49).

8. 3D Solution for Piezoelectric Rectangular Plate

Here, we consider a piezoelectric laminated rectangular plate subjected to thermal loading. The boundary conditions for the simply supported plate whose edges are electrically grounded and maintained at the reference temperature are written as:

$$\begin{aligned}
\Theta^{(n)} &= \varphi^{(n)} = \sigma_{11}^{(n)} = u_2^{(n)} = u_3^{(n)} = 0 \text{ at } x_1 = 0 \text{ and } x_1 = a,\\
\Theta^{(n)} &= \varphi^{(n)} = \sigma_{22}^{(n)} = u_1^{(n)} = u_3^{(n)} = 0, \text{ at } x_2 = 0 \text{ and } x_2 = b,
\end{aligned} \tag{68}$$

where a and b are the plate dimensions. To satisfy boundary conditions, we search the analytical solution of the problem by a method of double Fourier series expansion:

$$\Theta^{(n)i_n} = \sum_{r,s} \Theta_{rs}^{(n)i_n} \sin\frac{r\pi x_1}{a} \sin\frac{s\pi x_2}{b}, \tag{69}$$

$$\varphi^{(n)i_n} = \sum_{r,s} \varphi_{rs}^{(n)i_n} \sin\frac{r\pi x_1}{a} \sin\frac{s\pi x_2}{b},$$

$$u_1^{(n)i_n} = \sum_{r,s} u_{1rs}^{(n)i_n} \cos\frac{r\pi x_1}{a} \sin\frac{s\pi x_2}{b}, \tag{70}$$

$$u_2^{(n)i_n} = \sum_{r,s} u_{2rs}^{(n)i_n} \sin\frac{r\pi x_1}{a} \cos\frac{s\pi x_2}{b},$$

$$u_3^{(n)i_n} = \sum_{r,s} u_{3rs}^{(n)i_n} \sin\frac{r\pi x_1}{a} \sin\frac{s\pi x_2}{b}, \tag{71}$$

where r and s are the wave numbers in plane directions.

Using Fourier series (69), (70), and (71) in Eqs. (34) and (47) and accounting for relations (10), (11), (19), (20), (26), (27), (28), (30), (36), (41), (43), (52), (53), and (54), one derives:

$$J = \sum_{r,s} J_{rs}\left(\Theta_{rs}^{(n)i_n}\right), \tag{72}$$

Table 5. Results of the convergence study for a single-layer piezoelectric plate with $a/h = 10$ in the case of convective boundary conditions

I_1	$\bar{\Theta}(-0.5)$	$\bar{\Theta}(0.5)$	$\bar{\varphi}(0.5)$	$\bar{u}_1(0.5)$	$\bar{u}_3(0.5)$	$\bar{\sigma}_{11}(0.5)$	$\bar{\sigma}_{13}(-0.25)$	$\bar{\sigma}_{33}(0)$	$\bar{D}_3(0)$	$\bar{q}_3(0.5)$	$\bar{\eta}(0.5)$
5	0.72894	0.90045	−10.953	−4.1311	2.8608	−6.9137	1.7532	−9.9104	−3.3167	−2.9865	5.6212
7	0.72894	0.90045	−10.953	−4.1311	2.8608	−6.7182	1.9635	2.0573	−3.3154	−2.9865	5.6212
9	0.72894	0.90045	−10.953	−4.1311	2.8608	−6.7182	1.9634	2.0579	−3.3154	−2.9865	5.6212
11	0.72894	0.90045	−10.953	−4.1311	2.8608	−6.7182	1.9634	2.0579	−3.3154	−2.9865	5.6212
Dube	0.7289	0.9004	−10.95	−4.131	2.861	−6.718					

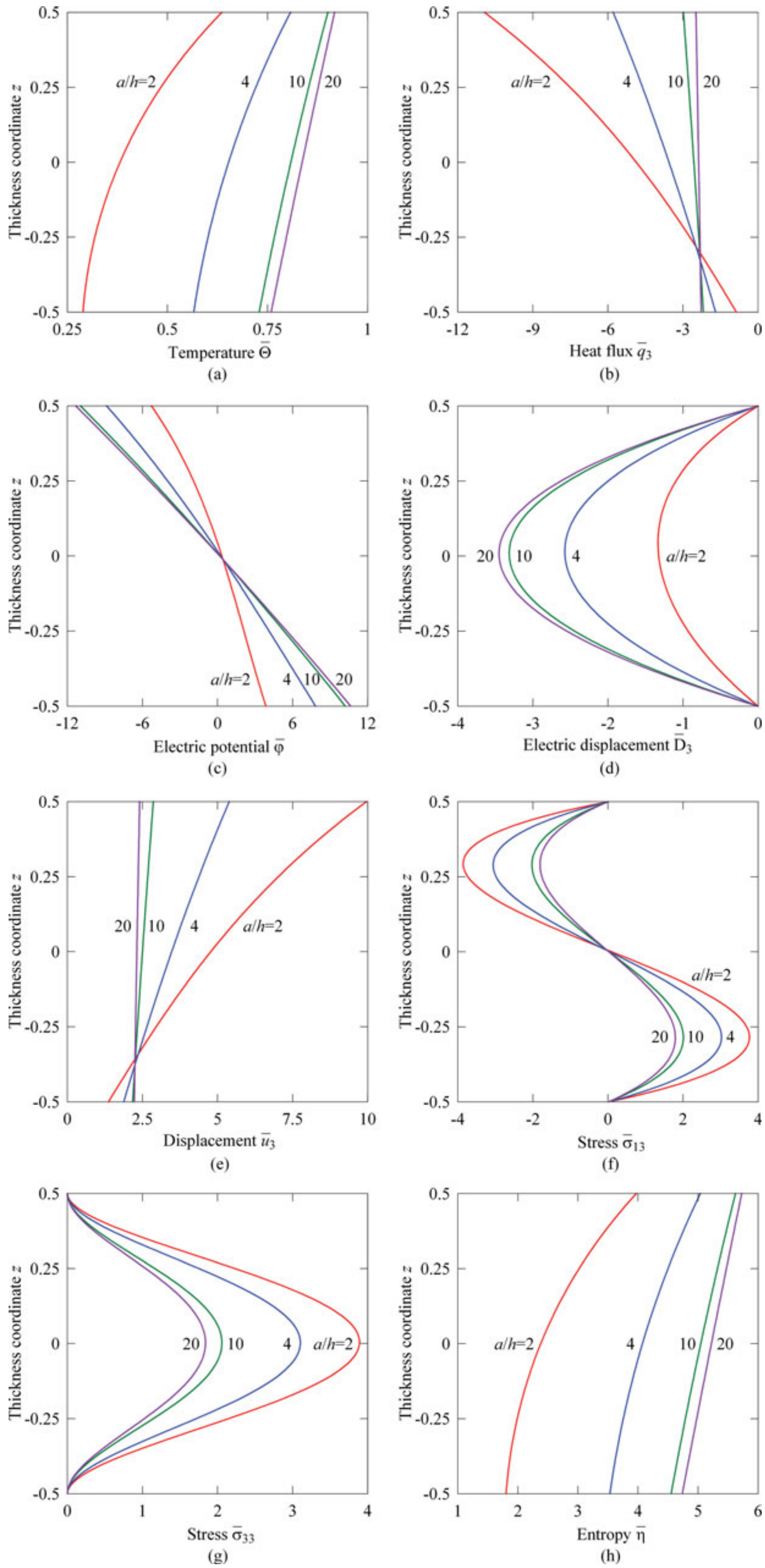

Fig. 2. Distributions of the temperature, heat flux, electric potential, electric displacement, transverse displacement, transverse stresses, and entropy through the thickness of the single-layer piezoelectric plate for $I_1 = 11$.

Table 6. Results of the convergence study for a two-layer piezoelectric plate with $a/h = 2$

I_n	$\bar{\Theta}(0)$	$\bar{\varphi}(0)$	$\bar{u}_1(0.5)$	$\bar{u}_3(0.5)$	$\bar{\sigma}_{11}(0.5)$	$\bar{\sigma}_{12}(0.5)$	$\bar{\sigma}_{13}(0)$	$\bar{\sigma}_{33}(0)$	$\bar{D}_3(0)$	$\bar{q}_3(0)$	$\bar{\eta}(0.5)$
3	0.60597	3.3660	−2.3924	10.317	−4.8826	−5.0768	1.6475	−2.3110	10.220	−3.0893	6.2427
							1.4076	−3.8790	−0.38923	−2.6675	
5	0.60583	3.3689	−2.3801	10.215	−4.6437	−5.0506	1.3421	−1.7144	−0.17554	−3.3443	6.2428
							1.3515	−1.6464	−0.31134	−3.3422	
7	0.60583	3.3689	−2.3801	10.215	−4.6431	−5.0506	1.3549	−1.6483	−0.30981	−3.3465	6.2428
							1.3500	−1.6475	−0.31035	−3.3465	
9	0.60583	3.3689	−2.3801	10.215	−4.6432	−5.0506	1.3501	−1.6477	−0.31034	−3.3465	6.2428
							1.3501	−1.6477	−0.31035	−3.3465	
11	0.60583	3.3689	−2.3801	10.215	−4.6432	−5.0506	1.3501	−1.6477	−0.31035	−3.3465	6.2428
							1.3501	−1.6477	−0.31035	−3.3465	

$$\Pi = \sum_{r,s} \Pi_{rs}\left(u_{irs}^{(n)i_n}, \varphi_{rs}^{(n)i_n}, \Theta_{rs}^{(n)i_n}\right). \tag{73}$$

Invoking variational equations (31) and (38), we arrive at two systems of linear algebraic equations:

$$\frac{\partial J_{rs}}{\partial \Theta_{rs}^{(n)i_n}} = 0, \tag{74}$$

$$\frac{\partial \Pi_{rs}}{\partial u_{irs}^{(n)i_n}} = 0, \quad \frac{\partial \Pi_{rs}}{\partial \varphi_{rs}^{(n)i_n}} = 0 \tag{75}$$

of orders K and $4K$, respectively, where $K = \sum_n I_n - N + 1$. The linear system (74) is solved first by a method of Gaussian elimination. Next, the linear system (75) is solved using the same method.

The described algorithm was performed with the Symbolic Math Toolbox, which incorporates symbolic computations into the numeric environment of MATLAB. This gives an opportunity to obtain the 3D exact solutions of thermoelectroelasticity for piezoelectric laminated rectangular plates with a specified accuracy.

As a numerical example, we consider a two-layer square plate subjected to the sinusoidally distributed temperature loading on the top surface, whereas the bottom surface is maintained at the reference temperature. The plate with equal thicknesses $h_1 = h_2 = h/2$ is composed of PZT-5A (lower layer) and cadmium selenide (upper layer) polarized in the thickness direction. It is assumed that both outer surfaces are electroded and grounded. Thus, the boundary conditions on the top and bottom surfaces can be written as:

$$\begin{aligned}
&\Theta^{(2)} = \Theta_0 \sin\frac{\pi x_1}{a} \sin\frac{\pi x_2}{b},\ \varphi^{(2)} = \sigma_{13}^{(2)} = \sigma_{23}^{(2)} = \sigma_{33}^{(2)} \\
&\quad = 0 \text{ at } x_3 = h/2, \\
&\Theta^{(1)} = \varphi^{(1)} = \sigma_{13}^{(1)} = \sigma_{23}^{(1)} = \sigma_{33}^{(1)} = 0 \text{ at } x_3 = -h/2,
\end{aligned} \tag{76}$$

where $a = b = 1\text{m}$, $\Theta_0 = 1\text{K}$, and $T_0 = 293\text{K}$. The material properties of PZT-5A and cadmium selenide are presented in [8, 15, 36] and Table 1.

Further, it is convenient to introduce dimensionless variables at crucial points as follows:

$$\begin{aligned}
\bar{\Theta} &= \Theta(a/2, a/2, z)/\Theta_0, \\
\bar{q}_3 &= 10aq_3(a/2, a/2, z)/Sk_0\Theta_0, \\
\bar{\varphi} &= 10^3 d_0\varphi(a/2, a/2, z)/a\alpha_0\Theta_0, \\
\bar{D}_3 &= D_3(a/2, a/2, z)/d_0E_0\alpha_0\Theta_0, \\
\bar{u}_1 &= 10u_1(0, a/2, z)/a\alpha_0\Theta_0, \\
\bar{u}_3 &= 100u_3(a/2, a/2, z)/Sa\alpha_0\Theta_0, \\
\bar{\sigma}_{11} &= 10\sigma_{11}(a/2, a/2, z)/E_0\alpha_0\Theta_0, \\
\bar{\sigma}_{12} &= 10\sigma_{12}(0, 0, z)/E_0\alpha_0\Theta_0, \\
\bar{\sigma}_{13} &= 10S\sigma_{13}(0, a/2, z)/E_0\alpha_0\Theta_0, \\
\bar{\sigma}_{33} &= 10S^2\sigma_{33}(a/2, a/2, z)/E_0\alpha_0\Theta_0, \\
\bar{\eta} &= 10^{-3}\eta(a/2, a/2, z)/E_0\alpha_0^2\Theta_0,\ S = a/h,\ z = x_3/h.
\end{aligned} \tag{77}$$

The reference material data α_0, k_0, d_0, and E_0 are given in a previous section.

Table 7. Results of the convergence study for a two-layer piezoelectric plate with $a/h = 10$

I_n	$\bar{\Theta}(0)$	$\bar{\varphi}(0)$	$\bar{u}_1(0.5)$	$\bar{u}_3(0.5)$	$\bar{\sigma}_{11}(0.5)$	$\bar{\sigma}_{12}(0.5)$	$\bar{\sigma}_{13}(0)$	$\bar{\sigma}_{33}(0)$	$\bar{D}_3(0)$	$\bar{q}_3(0)$	$\bar{\eta}(0.5)$
3	0.86748	6.6728	−2.8460	6.2762	−1.7075	−6.0394	1.6735	−6.5647	1.8313	−3.5125	6.2434
							3.3784	−8.2434	−1.8259	−3.5162	
5	0.86748	6.6726	−2.8455	6.2730	−1.6988	−6.0384	2.7117	−6.3918	−1.8001	−3.5268	6.2434
							2.7139	−6.3860	−1.8020	−3.5268	
7	0.86748	6.6726	−2.8455	6.2730	−1.6989	−6.0384	2.7132	−6.3876	−1.8020	−3.5268	6.2434
							2.7132	−6.3876	−1.8020	−3.5268	
9	0.86748	6.6726	−2.8455	6.2730	−1.6989	−6.0384	2.7132	−6.3876	−1.8020	−3.5268	6.2434
							2.7132	−6.3876	−1.8020	−3.5268	

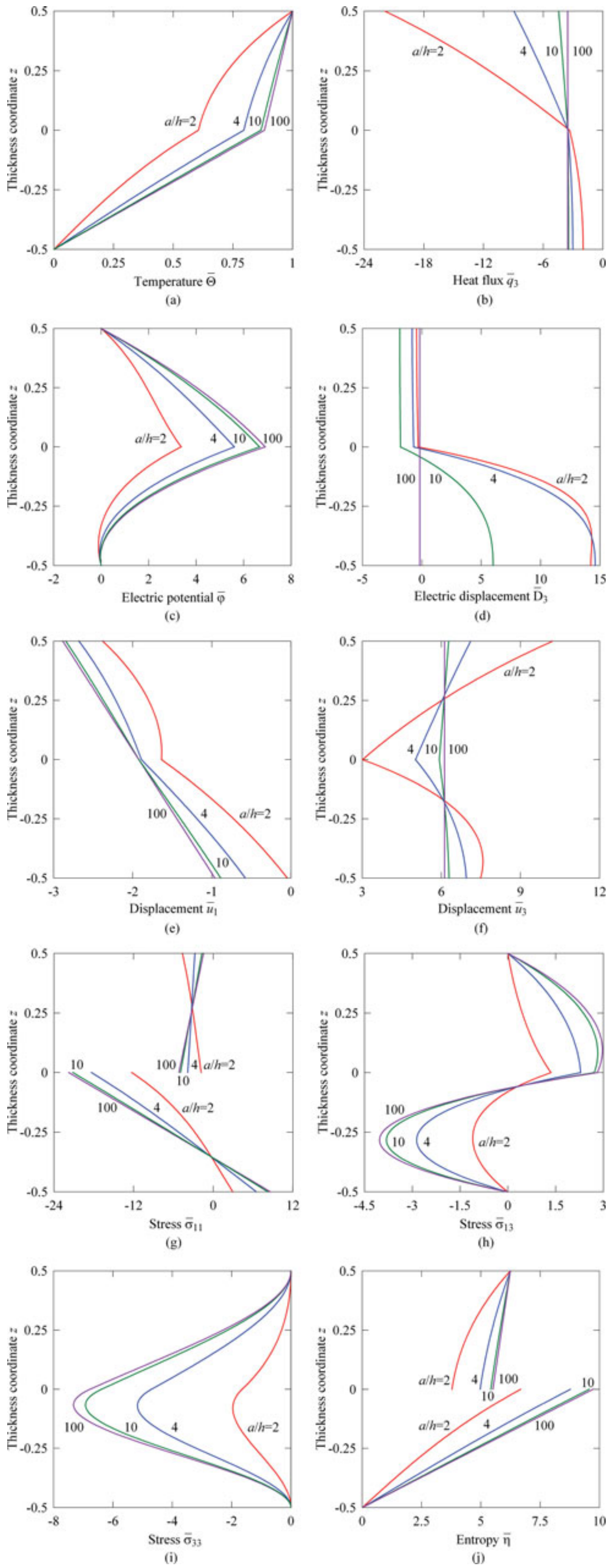

Fig. 3. Distributions of the temperature, heat flux, electric potential, electric displacement, displacements, stresses, and entropy through the thickness of the two-layer piezoelectric plate for $I_1 = I_2 = 9$.

Tables 6 and 7 show again the high potential of the SaS method, which yields the exact solution of 3D thermoelectroelasticity for piezoelectric laminated rectangular plates with a prescribed accuracy by using the sufficiently large number of SaS inside layers I_1 and I_2. Figure 3 presents through-the-thickness distributions of the temperature, heat flux, electric potential, electric displacement, displacements, stresses, and entropy for different slenderness ratios a/h employing nine SaS for each layer. It is seen that the boundary conditions for transverse stresses on the bottom and top surfaces and the continuity conditions for transverse components of the heat flux, electric displacement, and stress tensor at the layer interface are satisfied exactly. As we remember, these functions can be easily found via constitutive equations (35), (48), and (49).

9. Conclusions

An efficient method of solving the steady-state problem of 3D thermoelectroelasticity for piezoelectric laminated plates has been proposed. It is based on the new method of SaS located at Chebyshev polynomial nodes inside the layers and interfaces as well. The analysis of piezoelectric plates is based on the 3D constitutive equations and gives an opportunity to obtain exact 3D solutions of piezoelectricity for thick and thin plates with a specified accuracy.

Funding

This work was supported by the Russian Ministry of Education and Science under Grant No. 9.137.2014/K and by the Russian Foundation for Basic Research under Grant No. 13-01-00155.

References

[1] T.R. Tauchert, F. Ashida, N. Noda, S. Adali, and V. Verijenko, Developments in thermopiezoelasticity with relevance to smart composite structures, Compos. Struc., vol. 48, pp. 31–38, 2000.

[2] C.P. Wu, K.H. Chiu, and Y.M. Wang, A review on the three-dimensional analytical approaches of multilayered and functionally graded piezoelectric plates and shells, Comput., Mater. & Contin. vol. 8, pp. 93–132, 2008.

[3] B.F. Vlasov, On the bending of a rectangular thick plate, Trans. Moscow State Univ., vol. 2, pp. 25–31, 1957.

[4] N.J. Pagano, Exact solutions for composite laminates in cylindrical bending, J. Compos. Mater., vol. 3, pp. 398–411, 1969.

[5] N.J. Pagano, Exact solutions for rectangular bidirectional composites and sandwich plates, J. Compos. Mater., vol. 4, pp. 20–34, 1970.

[6] G.M. Kulikov, and S.V. Plotnikova, Solution of statics problems for a three-dimensional elastic shell, Doklady Phys., vol. 56, pp. 448–451, 2011.

[7] G.M. Kulikov, and S.V. Plotnikova, On the use of sampling surfaces method for solution of 3D elasticity problems for thick shells, ZAMM—J. Appl. Math. Mech., vol. 92, pp. 910–920, 2012.

[8] G.P. Dube, S. Kapuria, and P.C. Dumir, Exact piezothermoelastic solution of simply-supported orthotropic flat panel in cylindrical bending, Int. J. Mech. Sci., vol. 38, pp. 1161–1177, 1996.

[9] S. Kapuria, G.P. Dube, and P.C. Dumir, Exact piezothermoelastic solution for simply supported laminated flat panel in cylindrical bending, ZAMM—J. Appl. Math. Mech., vol. 77, pp. 281–293, 1997.
[10] F. Shang, Z. Wang, and Z. Li, Analysis of thermally induced cylindrical flexure of laminated plates with piezoelectric layers, Composites Part B, vol. 28, pp. 185–193, 1997.
[11] Y. Ootao, and Y. Tanigawa, Three-dimensional transient piezothermoelasticity for a rectangular composite plate composed of cross-ply and piezoelectric laminae, Int. J. Eng. Sci., vol. 38, pp. 47–71, 2000.
[12] C. Zhang, Y.K. Cheung, S. Di, and N. Zhang, The exact solution of coupled thermoelectroelastic behavior of piezoelectric laminates, Comput. Struc., vol. 80, pp. 1201–1212, 2002.
[13] K. Xu, A.K. Noor, and Y.Y. Tang, Three-dimensional solutions for coupled thermoelectroelastic response of multilayered plates, Comput. Meth. Appl. Mech. Eng., vol. 126, pp. 355–371, 1995.
[14] J.Q. Tarn, A state space formalism for piezothermoelasticity, Int. J. Solids Struc., vol. 39, pp. 5173–5184, 2002.
[15] S.S. Vel and R.C. Batra, Generalized plane strain thermopiezoelectric analysis of multilayered plates, J. Therm. Stresses, vol. 26, pp. 353–377, 2003.
[16] Z. Zhong and E.T. Shang, Exact analysis of simply supported functionally graded piezothermoelectric plates, J. Intel. Mater. Sys. Struc., vol. 16, pp. 643–651, 2005.
[17] Z.Q. Cheng and R.S. Batra, Three-dimensional asymptotic scheme for piezothermoelastic laminates, J. Therm. Stresses, vol. 23, pp. 95–110, 2000.
[18] G.M. Kulikov and S.V. Plotnikova, Exact 3D stress analysis of laminated composite plates by sampling surfaces method, Compos. Struc., vol. 94, pp. 3654–3663, 2012.
[19] G.M. Kulikov and S.V. Plotnikova, Advanced formulation for laminated composite shells: 3D stress analysis and rigid-body motions, Compos. Struc., vol. 95, pp. 236–246, 2013.
[20] G.M. Kulikov and S.V. Plotnikova, Three-dimensional exact analysis of piezoelectric laminated plates via a sampling surfaces method, Int. J. Solids Struc., vol. 50, pp. 1916–1929, 2013.
[21] G.M. Kulikov and S.V. Plotnikova, A sampling surfaces method and its application to three-dimensional exact solutions for piezoelectric laminated shells, Int. J. Solids Struc., vol. 50, pp. 1930–1943, 2013.
[22] G.M. Kulikov and A.A. Mamontov, Three-dimensional thermoelastic analysis of laminated anisotropic plates, Trans. Tambov State Tech. Univ., vol. 19, pp. 853–863, 2013.
[23] G.M. Kulikov and S.V. Plotnikova, Heat conduction analysis of laminated shells by a sampling surfaces method, Mech. Res. Commun., vol. 55, pp. 59–65, 2014.
[24] G.M. Kulikov, Refined global approximation theory of multilayered plates and shells, J. Eng. Mech., vol. 127, pp. 119–125, 2001.
[25] G.M. Kulikov and E. Carrera, Finite deformation higher-order shell models and rigid-body motions, Int. J. Solids Struc., vol. 45, pp. 3153–3172, 2008.
[26] Y.K. Cheung and C.P. Jiang, Finite layer method in analyses of piezoelectric composite laminates, Comput. Meth. Appl. Mech. Eng., vol. 191, pp. 879–901, 2001.
[27] G. Akhras and W.C. Li, Three-dimensional static, vibration and stability analysis of piezoelectric composite plates using a finite layer method, Smart Mater. Struc., vol. 16, pp. 561–569, 2007.
[28] G. Akhras and W.C. Li, Three-dimensional thermal buckling analysis of piezoelectric antisymmetric angle-ply laminates using finite layer method, Compos. Struc., vol. 92, pp. 31–38, 2010.
[29] C.P. Wu and Y.T. Chang, A unified formulation of RMVT-based finite cylindrical layer methods for sandwich circular hollow cylinders with an embedded FGM layer, Composites Part B, vol. 43, pp. 3318–3333, 2012.
[30] C.P. Wu and C.H. Kuo, A unified formulation of PVD-based finite cylindrical layer methods for functionally graded material sandwich cylinders, Appl. Math. Model., vol. 37, pp. 916–938, 2013.
[31] J.N. Reddy, Mechanics of Laminated Composite Plates and Shells: Theory and Analysis (2nd ed.), CRC Press, Boca Raton, FL, 2004.
[32] E. Carrera, Theories and finite elements for multilayered, anisotropic, composite plates and shells, Arch. Comput. Meth. Eng., vol. 9, pp. 1–60, 2002.
[33] E. Carrera, Theories and finite elements for multilayered plates and shells: A unified compact formulation with numerical assessment and benchmarking, Arch. Comput. Meth. Eng., vol. 10, pp. 215–296, 2003.
[34] E. Carrera, S. Brischetto, and P. Nali, Plates and Shells for Smart Structures: Classical and Advanced Theories for Modeling and Analysis, John Wiley & Sons Ltd., London, 2003.
[35] R.L. Burden and J.D. Faires, *Numerical Analysis (Ninth ed.)*, Brooks/Cole, Cengage Learning, Boston, MA, 2010.
[36] O. Madelung, Semiconductors: Data Handbook (3rd ed.), Springer, Berlin, 2004.